

Highly anisotropic Dirac fermion and spin transport properties in Cu-graphane

Chao Wu(吴超), Lichuan Zhang(张礼川), Lin Xia(夏霖), Dong Hao(郝东), Shiqi Li(李仕琪),Lizhi Zhang(张礼智), Yuee Xie(谢月娥), and Yuanping Chen(陈元平)

Citation: Chin. Phys. B, 2023, 32 (**8**): 087104. DOI: 10.1088/1674-1056/accff1
Journal homepage: http://cpb.iphy.ac.cn; http://iopscience.iop.org/cpb

What follows is a list of articles you may be interested in

Coexistence of giant Rashba spin splitting and quantum spin Hall effect in H-Pb-F

Wenming Xue(薛文明), Jin Li(李金), Chaoyu He(何朝宇), Tao Ouyang(欧阳滔), Xiongying Dai(戴雄英), and Jianxin Zhong(钟建新)

Chin. Phys. B, 2023, 32 (**3**): 037101. DOI: 10.1088/1674-1056/aca7eb

Influence of thickness on current-induced magnetization switching in $L1_0$-FePt single layer

Shi-Qi Zheng(郑诗琪), Kang-Kang Meng(孟康康), Zhen-Guo Fu(付振国), Ji-Kun Chen(陈吉堃), Jun Miao(苗君), Xiao-Guang Xu(徐晓光), and Yong Jiang(姜勇)

Chin. Phys. B, 2021, 30 (**10**): 107101. DOI: 10.1088/1674-1056/ac0a62

Recent progress on excitation and manipulation of spin-waves in spin Hall nano-oscillators

Liyuan Li(李丽媛), Lina Chen(陈丽娜), Ronghua Liu(刘荣华), and Youwei Du(都有为)

Chin. Phys. B, 2020, 29 (**11**): 117102. DOI: 10.1088/1674-1056/abaed5

Giant interface spin-orbit torque in NiFe/Pt bilayers

Shu-Fa Li(李树发), Tao Zhu(朱涛)

Chin. Phys. B, 2020, 29 (**8**): 087102. DOI: 10.1088/1674-1056/ab9292

Some corrections to the Thomas–Fermi theory

Janusz Chrzanowski

Chin. Phys. B, 2013, 22 (**8**): 087101. DOI: 10.1088/1674-1056/22/8/087101

Highly anisotropic Dirac fermion and spin transport properties in Cu-graphane

Chao Wu(吴超)[1,2], Lichuan Zhang(张礼川)[1,2,†], Lin Xia(夏霖)[1,2], Dong Hao(郝东)[1,2], Shiqi Li(李仕琪)[1,2], Lizhi Zhang(张礼智)[3], Yuee Xie(谢月娥)[1,2,‡], and Yuanping Chen(陈元平)[1,2]

[1] *School of Physics and Electronic Engineering, Jiangsu University, Zhenjiang* 212013, *China*
[2] *Jiangsu Engineering Research Center on Quantum Perception and Intelligent, Detection of Agricultural Information, Zhenjiang* 212013, *China*
[3] *National Center for Nanoscience and Technology of China, Beijing* 100190, *China*

(Received 12 March 2023; revised manuscript received 20 April 2023; accepted manuscript online 25 April 2023)

Inspired by the successful synthesis of hHv-graphane [*Nano Lett.* **15** 903 (2015)], a new two-dimensional (2D) Janus material Cu-graphane is proposed based on the first-principles calculations. Without the spin–orbit coupling (SOC) effect, Cu-graphane is a Dirac semimetal with a highly anisotropic Dirac cone, whose Fermi velocity ranges from 0.12×10^5 m/s to 2.9×10^5 m/s. The Dirac cone near the Fermi level can be well described with an extended 2D Dirac model Hamiltonian. In the presence of the SOC effect, band splitting is observed around the Fermi level, and a large intrinsic spin Hall conductivity (ISHC) with a maximum value of 346 $(\hbar/e)$ S/cm is predicted. Moreover, the spin Hall transport can be regulated by slightly adjusting the Fermi energy, e.g., grid voltage or chemical doping. Our work not only proposes a new 2D Janus material with a highly anisotropic Dirac cone and a large ISHC, but also reveals that a large ISHC may exist in some Dirac systems.

Keywords: graphane, anisotropic Dirac fermion, Janus, spin Hall effect

PACS: 71.70.Ej, 72.25.–b, 73.22.–f, 81.05.Zx **DOI:** 10.1088/1674-1056/accff1

1. Introduction

Since its first successful synthesis, graphene has caught widespread attention for its mechanical stability, high carrier mobility, isotropic Dirac fermions, and other properties.[1–4] In the graphene family, the graphane, i.e., hydrogenated graphene, which is predicated as an insulator,[5] has been prepared experimentally with different methods since 2009.[6–9] Among them, the graphane with honeycomb H vacancies of several ordered configurations, so-called hHv-graphane, has been observed on the Cu(111) surface via scanning tunneling microscopy.[10] The hHv-graphane provides a perfect platform to bond with other atoms due to its dangling bonds, and some systems, e.g., As-graphane[11] and Sn-graphane,[12] have been predicted, which hold unique properties including quantum spin Hall effect (SHE), tunable spin transport properties, and room-temperature quantum anomalous Hall effect. The *M*-graphane (M = metal atom) is a Janus system with broken mirror symmetry, suggesting its candidate applications in electronic, optoelectronic, nonlinear optics, and catalysis fields, etc.[13–17] However, in these new Janus systems, only As-graphane and Sn-graphane have been studied, which motivates us to investigate new systems constructed by hHv-graphane and transition metal atoms.

In this work, we combined the transition metal Cu atom with hHv-graphane to construct a new two-dimensional (2D) Janus material, Cu-graphane. Through phonon dispersion and *ab initio* molecular dynamics simulations, we demonstrated its dynamic and thermal stability. Using comprehensive density functional theory (DFT) calculations, we investigated its electronic band structure and spin transport characteristic. When the SOC is ignored, we discovered an ultrahigh anisotropic Dirac cone at an asymmetric point between the K and Γ points near the Fermi level, characterized by a wide range of Fermi velocities from 0.12×10^5 m/s to 2.9×10^5 m/s along different directions in k-space. Besides, this Dirac point can be perfectly described with an effective 2×2 Dirac Hamiltonian multiplied by a spatial rotation matrix. When the SOC is introduced, the band structure splits, and Dirac points are slightly gapped. Besides, its SHE is also investigated based on the semi-classical theory. A large intrinsic spin Hall conductivity (ISHC) with 346 $(\hbar/e)$ S/cm is obtained, which can be modulated via grid voltage or electron–hole doping. Our work not only proposes a new material with anisotropic Dirac points and large ISHC, but also investigates the modulation of SHE.

2. Computational details

All density functional theory calculations are adopted by the Vienna *ab initio* simulation package (VASP)[18] with the generalized gradient approximation (GGA) of Perdew–Burke–Ernzerhof (PBE)[19] for the exchange–correlation potential. The interaction between the electron and nuclei is expressed with the projector-augmented wave (PAW) method.[20] 700 eV

†Corresponding author. E-mail: Lichuan.zhang@ujs.edu.cn
‡Corresponding author. E-mail: yueex@ujs.edu.cn

© 2023 Chinese Physical Society and IOP Publishing Ltd

is selected for the kinetic energy cutoff of the plane wave function and 10^{-7} is set as the energy convergence threshold. The Brillouin zone (BZ) is sampled with $15 \times 15 \times 1$ Gamma-centered Monkhorst–Pack grids.[21] In all calculations, the vacuum layer is selected as 20 Å, the shape and volume for each cell are fully optimized and the maximum force on each atom is less than 0.001 eV/Å. The phonon dispersion curve is calculated with the code PHONOPY[22,23] by a supercell $4 \times 4 \times 1$. The first-principles molecular dynamics (MD) simulations are performed with a 3×3 supercell. Coulomb and exchange interactions of the localized d orbitals in the Cu element are tested with the DFT + U method proposed by Dudarev *et al.*[24,25] The Berry curvature and ISHC[26] are performed by the maximally localized Wannier function method,[27] implemented in the WANNIER90 package.[28] The ISHC is obtained from the Kubo formula[29]

$$\sigma_{xy} = -\frac{e^2}{\hbar}\frac{1}{VN_k^3}\sum_k \Omega_{xy}^{s_z}(\boldsymbol{k}), \tag{1}$$

where V is the primitive cell volume, N_k^3 is the number of $\boldsymbol{k}$ points in the BZ, and the $\boldsymbol{k}$-resolved term is

$$\Omega_{xy}^{s_z}(\boldsymbol{k}) = \sum_n f_{n\boldsymbol{k}}\Omega_{n,xy}^{s_z}(\boldsymbol{k}), \tag{2}$$

and the so-called spin-Berry-curvature-like term is[30]

$$\Omega_{n,xy}^{s_z}(\boldsymbol{k}) = \hbar^2 \sum_{m\neq n} \frac{-2\mathrm{Im}\left[\langle n\boldsymbol{k}|\frac{1}{2}\{\hat{j}_x^z, \hat{v}_x\}|m\boldsymbol{k}\rangle\langle m\boldsymbol{k}|\hat{v}_y|n\boldsymbol{k}\rangle\right]}{(E_{n\boldsymbol{k}} - E_{m\boldsymbol{k}})^2}, \tag{3}$$

where $E_{n\boldsymbol{k}}$ and $E_{m\boldsymbol{k}}$ are the eigenvalues of n-th and m-th bands for the $\boldsymbol{k}$-dependent Hamiltonian $H(\boldsymbol{k})$, respectively, and f_{nk} is the Fermi–Dirac distribution function. $\hat{j}_x^z = \frac{1}{2}\{\hat{s}_z, \hat{v}_x\}$ is the spin current operator, which is determined by the spin operator $\hat{s}_z = \frac{\hbar}{2}\hat{\sigma}_z$ and the velocity operator $\hat{v}_y = \frac{1}{\hbar}\frac{\partial H(\boldsymbol{k})}{\partial k_y}$.

In this work, the color map of $\Omega_{n,xy}^{s_z}(\boldsymbol{k})$ in Fig. 5 is defined as

$$\text{result} = \begin{cases} \mathrm{sgn}(x)\log_{10}|x|, & |x| > 10, \\ x/10, & |x| \leq 10, \end{cases} \tag{4}$$

where the function $\mathrm{sgn}(x)$ refers to the sign of x.

3. Results and discussion

3.1. Structure and stability

The schematic structure of Cu-graphane is shown in Fig. 1(a) with a top view and side view, respectively. Clearly, these Cu atoms form a monolayer honeycomb lattice above the graphane surface with a bond length of approximately 2.03 Å for Cu and C atoms, more crystal structure parameters can be seen in Table S1. As shown in Table S2, a large binding energy of 3.474 eV is obtained in Cu-graphane. The dashed line outlines the primitive cell of Cu-graphane with a lattice constant of approximately 4.465 Å. To demonstrate the stability of Cu-graphane, we calculate its phonon dispersion curve, and no imaginary frequencies are observed in Fig. 1(b). Besides, as shown in Figs. 1(c) and S1, we perform the first-principles MD simulations using a 3×3 supercell at 300 K, and the thermal dynamical stability is ensured.

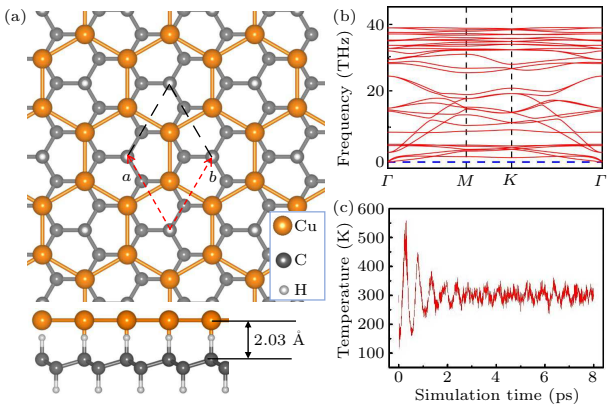


Fig. 1. Structure and stability analyses of Cu-graphane. (a) Schematic structure of the Cu-graphane with the top and side views, and the dashed lines outline the unit cell of Cu-graphane. (b) The phonon dispersion curves of Cu-graphane and (c) the *ab initio* molecular dynamics simulation with temperature of 300 K.

3.2. Band structure and anisotropic Dirac fermion without SOC

The band structure and the corresponding projected density of states (PDOS) for Cu-graphane are shown in Fig. 2(a). It is illustrated that the Dirac point, marked as B, exists at the Fermi level between the high-symmetry points Γ and K. Besides, a very small band gap of about 20 meV is obtained at position A between the high-symmetry points Γ and M. In the BZ, the positions of B and A are located at (0.1139, 0.1139, 0) and (0.2, 0, 0), respectively. As the structure holds the C_6 symmetry, Cu-graphane has six equivalent Dirac points. According to the PDOS and the partial charge density analyses in Fig. S2, these Dirac cones can be attributed to the overlap of valence band and conduction band, which are mainly contributed from the d_{z^2} orbital of Cu atoms and p_z orbital of their nearby C atoms. To demonstrate the precise band structure of Cu-graphane, the three-dimensional (3D) band structure near the Fermi level is drawn in Fig. 2(b). Compared to graphene or graphynes,[2,31,32] Dirac points in Cu-graphane exhibit huge anisotropic properties, and the band structure is similar to the nodal ring (shown in Figs. 2(c) and S4).

To uncover the ultrahigh anisotropic properties of Dirac fermions, the Fermi velocity of the Dirac point is calculated based on the linear dispersions. The Fermi velocity of the Dirac cone along different directions is shown in Fig. 3(a), and we can find that the Fermi velocity of electrons and holes almost has a reversal symmetry, which is consistent with the band structure. As shown in Figs. 3(b) and 3(c), the largest

velocity is obtained along the Γ–K direction (1.0×10^5 m/s, 2.9×10^5 m/s) and the minimum value exists perpendicular to the Γ–K direction (0.12×10^5 m/s, 0.18×10^5 m/s), where the maximum velocity is almost 10 times larger than the minimum velocity. Besides, the effective mass $2.4m_e$ for the hole and $1.2m_e$ for the electron are presented in Fig. 3(b).

To describe the highly anisotropic Dirac cone, an effective 2D Hamiltonian $H(\boldsymbol{k})$ is selected as[33–36]

$$H(\boldsymbol{k}) = \boldsymbol{h}(\boldsymbol{k})\cdot\boldsymbol{\sigma}, \tag{5}$$

with $\boldsymbol{h}(\boldsymbol{k}) = \left(k_x^2/(2m) - v_y k_y, v_x k_x, 0\right)$ and $\boldsymbol{\sigma} = (\sigma_x, \sigma_y, \sigma_z)$. Then, the energy dispersion around the Dirac cone can be expressed as

$$E = \begin{cases} \sqrt{\left(\frac{k_x^2}{2m_c} - v_y^c k_y\right)^2 + (v_x^c k_x)^2}, \\ -\sqrt{\left(\frac{k_x^2}{2m_v} - v_y^v k_y\right)^2 + (v_x^v k_x)^2}, \end{cases} \tag{6}$$

where the specific values of v_x^v, v_x^c, v_y^v, v_y^c, m_c, and m_v have been clearly marked in Figs. 3(b) and 3(c). The band structure of the model looks very similar to the 3D band structure of the first-principles, demonstrating that our model provides a perfect description of the *ab initio* results.

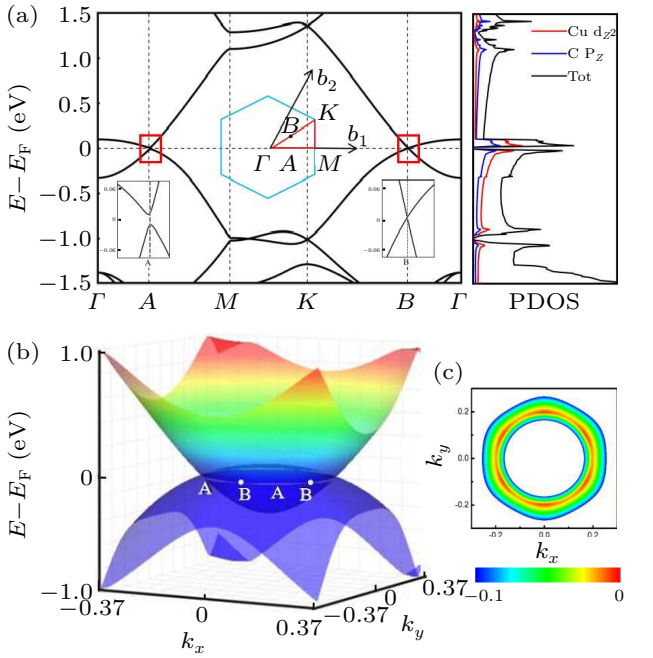


Fig. 2. Electronic band structure of Cu-graphane. (a) Band structure and PDOS of Cu-graphane. The middle inset illustrates the first BZ, and the bottom right and left corners indicate the zoom-in of the band structure around the *A* and *B* points, respectively. (b) The 3D band structure of valence and conduction bands near the Fermi level for Cu-graphane. (c) The 2D contour plat of the conduction band near the Fermi level in *k*-space. The unit cell of the color bar is in eV.

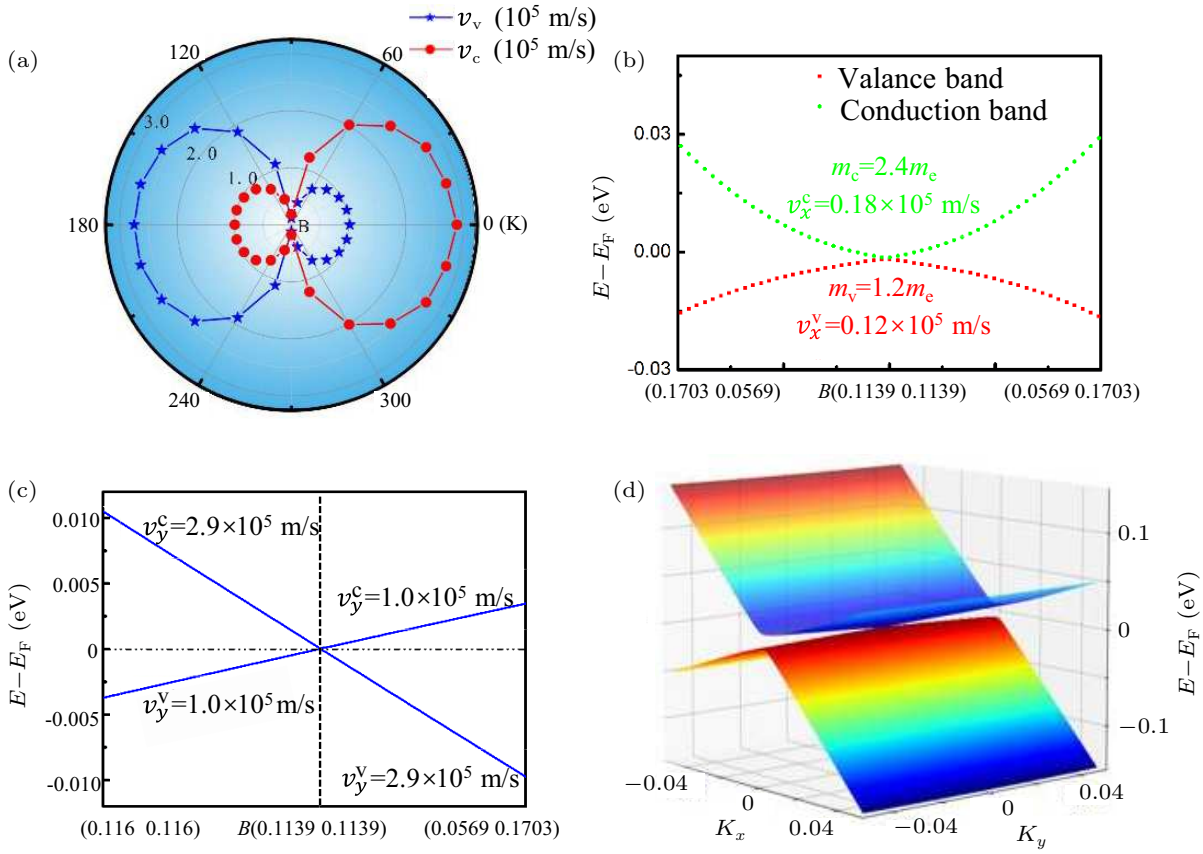


Fig. 3. Anisotropic properties of Dirac point in Cu-graphane. (a) The Fermi velocity of Dirac point for the valence band and conduction band as a function of the polarization angle θ. The $\theta = 0°$ corresponds to the *B*–*K* direction. The band structure around the Dirac point area with the path (b) perpendicular to the *B*–*K* direction, and (c) along the *K*–Γ direction. Fermi velocity and effective mass are marked respectively in panels (b) and (c). (d) The 3D plot of the low-energy dispersion with the fitted model.

In this work, the LSDA + U methods are adopted, and the results are shown in Fig. S5, demonstrating that the Hubbard U effect on the band structure is tiny. Meanwhile, the strain effect of Cu-graphane is also investigated, and the semimetal and semiconductor transformations are observed, as illustrated in Fig. S6.

3.3. Intrinsic spin Hall conductivity

In the previous part, we illustrate anisotropic Dirac points in Cu-graphane when the SOC is absent. The Cu-graphane is a Janus material, and the vertical mirror symmetry is broken, leading to a Rashba SOC.[37] In Fig. 4(a), the band structure is presented when the Rashba SOC is considered, and the band splitting is mainly observed around point A and Dirac point B. As the Rashba SOC can enhance the SHE,[38] we calculate the ISHC of Cu-graphane. The ISHC with the function of the Fermi energy (E_F) is presented in Fig. 4(b), with the Fermi level setting to zero energy. We can see that near the Fermi level, the minimum value of ISHC occurs when $E - E_F = E_2 = 0$ eV with the magnitude of 23.4 $(\hbar/e)$ S/cm. Besides, the ISHC increases sharply when the energy shifts away from E_2, and the maximum values occur at $E_1 = -0.093$ eV with 346 $(\hbar/e)$ S/cm and $E_3 = 0.022$ eV with 226 $(\hbar/e)$ S/cm, respectively. Compared to other 2D systems,[38–40] a big ISHC is not only obtained, but also can be regulated easily by the grid voltage or the electron/hole doping.

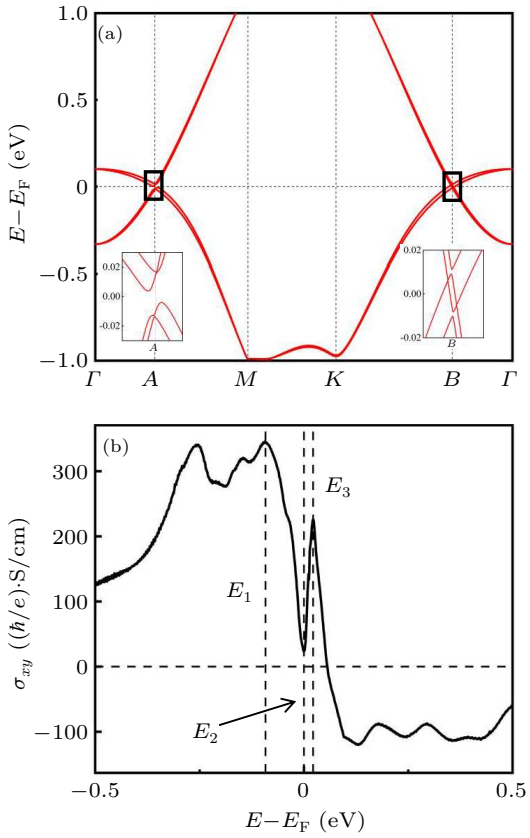


Fig. 4. The SOC effect for Cu-graphane. (a) Band structure of Cu-graphane in the presence of SOC. Insets of (a) indicate the zoomed illustration of the band structure around the area of A and B points, respectively. (b) The ISHC of Cu-graphane with the function of E_F.

To analyze the novel behavior of ISHC with E_F, we calculate the band-projected spin Berry curvature in Fig. 5(a), where these dotted lines correspond to the same energy marked in Fig. 4(b). As shown in Figs. 5(b)–5(d), the k-resolved spin Berry curvatures at E_1, E_2, and E_3 are shown in a slice of the 2D BZ and in a contour plot, where blue and red colors indicate negative and positive contributions, respectively. It is indicated that the regulation of E_F from E_2 to E_1 can significantly change the value of $\Omega_{xy}^{s_z}(\boldsymbol{k})$, and the shape of $\Omega_{xy}^{s_z}(\boldsymbol{k})$ evolutes from a ring with the positive and negative contributions in an alternate way to an outer ring with positive contributions and an inner ring with weak contributions in the first BZ. Similarly, when E_F changes from E_2 to E_3, the shape of $\Omega_{xy}^{s_z}(\boldsymbol{k})$ becomes an outer ring with the alternate positive and negative contributions marked by red and blue colors, and an inner ring with totally positive contributions. Obviously, when the E_F shifts from E_2 to E_1/E_3, the total contribution of $\Omega_{xy}^{s_z}(\boldsymbol{k})$ in the first BZ increases, leading to a rising trend of ISHC.

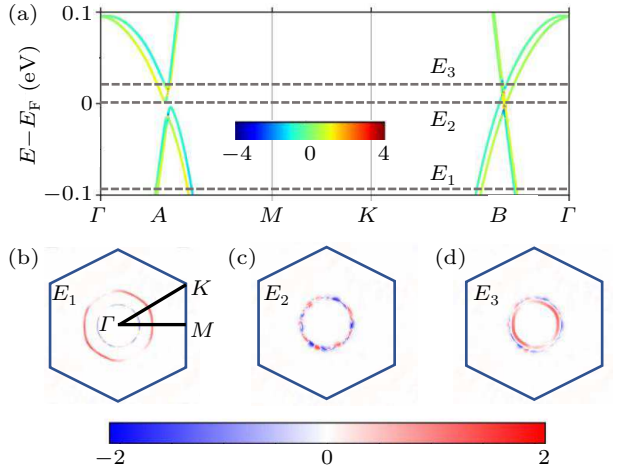


Fig. 5. The spin Berry curvature. (a) Band structure of Cu-graphane projected by spin Berry curvatures on a log scale around the Fermi level. (b)–(d) The k-resolved spin Berry curvature on a log scale in the contour plot of the 2D BZ at E_1, E_2, and E_3 in the monolayer Cu-graphane, respectively. The red and blue colors indicate the positive and negative contributions, respectively.

4. Conclusion

Inspired by the experiment, we construct a new stable 2D Janus material Cu-graphane with novel band structure and perfect spin polarization transport properties. In the first BZ, we find six highly anisotropic Dirac points located in the Γ–K (K') path, and the maximum Fermi velocity (B–K direction) is about 10 times larger than the minimum one (perpendicular to the B–K direction), which can be perfectly repeated by an effective Hamiltonian model. We find that this Dirac system is a quasi-nodal ring system, as the maximum band gap between the conduction band and valence is only about 20 meV. When

the Rashba SOC is considered, we find that Cu-graphane has perfect spin polarized transport characteristics. A large ISHC is predicated, which can be modulated by adjusting the grid voltage or the electron/hole doping. Our study provides a new stable Janus material, which has potential application in spintronics, and suggests that the large and easily regulated ISHC may exist in Dirac systems.[41]

Acknowledgments

The authors thank Prof. Jiaren Yuan of Nanchang University for the helpful discussions. Project supported by the National Natural Science Foundation of China (Grant Nos. 12074150, 12174157, 12174158, and 11874314), the Innovation and Entrepreneurship Talent Project of Jiangsu Province of China, the Scientific Research Startup of Jiangsu University (Grant No. 5501710001), and the College Students' Innovation Training Program of Jiangsu Province of China (Grant No. 202110299123Y).

References

[1] Novoselov K S, Geim A K, Morozov S V, Jiang D, Zhang Y, Dubonos S V, Grigorieva I V and Firsov A A 2004 *Science* **306** 666
[2] Geim A K and Novoselov K S 2007 *Nat. Mater.* **6** 183
[3] Bolotin K I, Sikes K J, Jiang Z, Klima M, Fudenberg G, Hone J, Kim P and Stormer H L 2008 *Solid State Commun.* **146** 351
[4] Zhang Y, Jia L, Chen Y, He L and Wang Y 2022 *Chin. Phys. B* **31** 087301
[5] Sofo J O, Chaudhari A S and Barber G D 2007 *Phys. Rev. B* **75** 153401
[6] Elias D C, Nair R R, Mohiuddin T M G, Morozov S V, Blake P, Halsallm P, Ferrari A C, Boukhvalov D W, Katsnelson M I, Geim A K and Novoselov K S 2009 *Science* **323** 610
[7] Chen H, Bao D L, Wang D, Que Y, Xiao W, Qian G, Guo H, Sun J, Zhang Y Y and Du S 2018 *Adv. Mater.* **30** 1801838
[8] Chen W, Zhu Z, Li S, Chen C and Yan L 2012 *Nanoscale* **4** 2124
[9] Eng A Y S, Poh H L, Sanek F, Marysko M, Matejkova S, Sofer Z and Pumera M 2013 *ACS Nano* **7** 5930
[10] Lin C, Feng Y, Xiao Y, Durr M, Huang X, Xu X, Zhao R, Wang E, Li X Z and Hu Z 2015 *Nano Lett.* **15** 903
[11] Zhang L Z, Zhai F, Jin K H, Cui B, Huang B, Wang Z, Lu J Q and Liu F 2017 *Nano Lett.* **17** 4359
[12] Zhang L, Park C and Yoon M 2020 *Nano Lett.* **20** 7186
[13] Zhang J, Jia S, Kholmanov I, Dong L, Er D, Chen W, Guo H, Jin Z, Shenoy V B, Shi L and Lou J 2017 *ACS Nano* **11** 8192
[14] Lu A Y, Zhu H, Xiao J, Chuu C P, Han Y, Chiu M H, Cheng C C, Yang C W, Wei K H, Yang Y, Wang Y, Sokaras D, Nordlund D, Yang P, Muller D A, Chou M Y, Zhang X and Li L J 2017 *Nat. Nanotechnol.* **12** 744
[15] Riis-Jensen A C, Deilmann T, Olsen T and Thygesen K S 2019 *ACS Nano* **13** 13354
[16] Xie S, Jin H, Wei Y and Wei S 2021 *Optik* **227** 166105
[17] Li X D, Yu Z D, Chen W P and Gong C D 2022 *Chin. Phys. B* **31** 110304
[18] Kresse G and Furthmuller J 1996 *Phys. Rev. B* **54** 11169
[19] Perdew J P, Burke K and Ernzerhof M 1996 *Phys. Rev. Lett.* **77** 3865
[20] Kresse G and Joubert D 1999 *Phys. Rev. B* **59** 1758
[21] Monkhorst H J and Pack J D 1976 *Phys. Rev. B* **13** 5188
[22] Parlinski K, Li Z Q and Kawazoe Y 1997 *Phys. Rev. Lett.* **78** 4063
[23] Togo A, Oba F and Tanaka I 2008 *Phys. Rev. B* **78** 134106
[24] Dudarev S L, Botton G A, Savrasov S Y, Humphreys C J and Sutton A P 1998 *Phys. Rev. B* **57** 1505
[25] Anisimov V I, Aryasetiawan F and Lichtenstein A I 1997 *J. Phys. Condens. Matter* **9** 767
[26] Sinova J, Valenzuela S O, Wunderlich J, Back C H and Jungwirth T 2015 *Rev. Mod. Phys.* **87** 1213
[27] Marzari N, Mostofi A A, Yates J R, Souza I and Vanderbilt D 2012 *Rev. Mod. Phys.* **84** 1419
[28] Pizzi G, Vitale V, Arita R, *et al.* 2020 *J. Phys. Condens. Matter* **32** 165902
[29] Zhou J, Qiao J, Bournel A and Zhao W 2019 *Phys. Rev. B* **99** 060408
[30] Gradhand M, Fedorov D V, Pientka F, Zahn P, Mertig I and Györff B L 2012 *J. Phys. Condens. Matter* **24** 213202
[31] Malko D, Neiss C, Vines F and Gorling A 2012 *Phys. Rev. Lett.* **108** 086804
[32] Zhang L Z, Wang Z F, Wang Z M, Du S X, Gao H J and Liu F 2015 *J. Phys. Chem. Lett.* **6** 2959
[33] Wang J, Deng S, Liu Z and Liu Z 2015 *Natl. Sci. Rev.* **2** 22
[34] Banerjee S, Singh R R P, Pardo V and Pickett W E 2009 *Phys. Rev. Lett.* **103** 016402
[35] Huang H, Liu Z, Zhang H, Duan W and Vanderbilt D 2015 *Phys. Rev. B* **92** 161115
[36] Asano K and Hotta C 2011 *Phys. Rev. B* **83** 245125
[37] Shanavas K V, Popović Z S and Satpathy S 2014 *Phys. Rev. B* **90** 165108
[38] Yu S B, Zhou M, Zhang D and Chang K 2021 *Phys. Rev. B* **104** 075435
[39] Feng W, Yao Y, Zhu W, Zhou J, Yao W and Xiao D 2012 *Phys. Rev. B* **86** 165108
[40] Guo G Y, Yao Y and Niu Q 2005 *Phys. Rev. Lett.* **94** 226601
[41] Yen Y and Guo G Y 2020 *Phys. Rev. B* **101** 064430